PCCP

Accepted Manuscript

ROYAL SOCIETY OF CHEMISTRY

www.rsc.org/pccp

Spectroscopic evidence of 3-hydroxyflavone sorption within MFI type zeolites: ESIPT and metal complexation

A. Moissette,* [a] M. Hureau,[a] A. Kokaislova,[a,b] A. Le Person,[a] J.P. Cornard,[a] I. De Waele,[a] I. Batonneau-Gener[c]

[a] *LASIR, UMR-CNRS 8516, Université de Lille, Sciences et Technologies, Bât. C5, Villeneuve d'Ascq cedex, France*

[b] *Department of analytical chemistry, Institute of Chemical Technology, Technická 5, 166 28 Praha 6 – Dejvice, Czech republic*

[c] *IC2MP-UMR 7285, Faculté des Sciences Fondamentales et Appliquées, Bât B27, 4 Rue Michel Brunet - TSA 51106, 86073 Poitiers cedex 9, France*

Abstract - Due to its chemical and photochemical properties and of its potential applications in numerous domains as molecular probe, 3-hydroxyflavone (3HF) is a molecule of high interest. In particular, the processes of intramolecular proton transfer in the excited state and of metallic complexation are known to be dependent on the chemical environment. In this context, the particular properties of zeolites make these microporous materials an environment adapted to study the reactivity of isolated molecules adsorbed in their porous void space. Thus, this report investigates the incorporation without any solvent of 3HF into the internal volume of various channel-type MFI zeolites. Using complementary techniques (Diffuse reflectance UV-vis absorption, Raman scattering, FTIR, fluorescence emission and molecular modelling), very different spectral behaviours are observed in totally dealuminated silicalite-1 and in Al rich MZSM-5 (M= H^+, Na^+, Zn^{2+}). In silicalite-1, the non-polar and non-protic internal micro-environment does not induce any valuable interaction between 3HF and the channel walls. Therefore the molecule shows easy tautomer formation upon excitation. Within HZSM-5, 3HF is adsorbed in close proximity of the acid proton of zeolite which inhibits the intramolecular proton transfer and then, only the normal form is observed at the excited state. For NaZSM-5, the spectral data show an intermediary behaviour due to aprotic but polar environment, in agreement with 3HF sorption in close proximity of the Na^+ extraframework cation. After mixing 3HF and ZnZSM-5, the spectral features clearly indicate metallic complexation of the guest molecule. The zeolite dependent reactivity reported here demonstrates the adsorption of the guest within the internal volume because the charge balancing cations which clearly control the reaction are principally located in the zeolite channels. The 3HF incorporation into the internal volume is proved by the decrease of the microporous volume observed by nitrogen adsorption-desorption isotherm measurements. The experimental data are confirmed by Monte Carlo molecular modelling which predicts also 3HF sorption in the zeolite channels in the proximity of charge compensating cations. Consequently, as the molecule dimensions are assumed to be slightly larger than the channel size, the flexibility of the molecule and the lattice deformation have to be considered to allow 3HF penetration into the zeolite void space.

Introduction

The molecules belonging to the flavonoid family are well-known for their photoprotective properties [1] and for their antioxidant activity [2]. Among flavonoids, 3-hydroxyflavone (3HF) is of particular interest because it can adopt different forms by proton transfer [3,4] depending on the environment polarity and on its capacity to form hydrogen bonds and its ability to chelate metals like Al(III), Pb(II), Cu(II), Zn(II). [5-10] Especially, the capacity of flavonoids to chelate metallic cations is of high importance to improve their antioxidant activity.[11] This molecule provides a valuable probe to investigate the local microenvironment and then, to get better knowledge of its properties, it is essential to investigate thoroughly the structural changes occurring upon the interactions induced by the surrounding media and upon photoexcitation. 3HF photoreactivity was widely studied in solution using various solvents [12-14] but also at a supramolecular level using assemblies like micelles [15], cyclodextrins [16,17], sol gel glasses [18,19], polysiloxanes [20], liposome membranes [21,22] and even colloidal suspensions of zeolite [23] corresponding to various aprotic or protic, and/or polar or apolar surrounding media. All these works showed that the excited state intramolecular proton transfer (ESIPT) taking place in 3HF is very dependent on the protic nature and polarity of the 3HF molecule environment (scheme 1). Chelation was also studied in several solvents and hydro-organic media such as water-ethanol and water-methanol. [5]

In that context, zeolites can indeed be considered as solid solvents as they provide an interesting micro-environment to investigate the reactivity of spectrally sensitive molecules like 3HF trapped on specific sites. The inner environment of zeolites is composed by a negatively charged framework and by charge compensating cations located in the microporous volume. Adsorbed molecules interact both with the framework oxygens and with the exchangeable cations. If this interaction is weak it can be considered as a solvent-type interaction. The exchangeable cations are only partially shielded by the negative charge of the lattice. As a consequence their electrostatic field in the micropores can be high. [24]

Due to restricted geometry and to the possibility of modulate the molecule surrounding by acting locally on the polarity and on the ability to create hydrogen bonding, different behaviours are expected upon guest incorporation into the host framework using various charge balancing cations with more or less polar and protic characters. In addition, at relatively low loading, the guest molecule dispersion is assumed to be high enough to prevent molecule-molecule interaction and to let us consider that the guest molecule is at the isolated state in a particular environment.

We report here the conspicuous spectral changes observed on incorporation without any solvent of 3HF into the internal void space of various channel type MFI zeolites. The different spectroscopic signatures reflect the key role of the confinement through interactions between the guest molecule, the pore walls and the charge compensating cation and give valuable information on the zeolite internal properties. The direct relation between the cation type and the polarity and/or acidity is highlighted by comparing the drastic changes observed on the spectra on adsorbing 3HF in totally dealuminated silicalite-1 and in Al rich MZSM-5 (M= H^+, Na^+, Zn^{2+}). In addition, molecular modelling data provide complementary information to address the preferential sorption sites and molecule conformation in the zeolite channels.

Experimental section

1. Materials. The purely siliceous MFI (silicalite-1) sample synthesized in fluoride medium was a gift from Dr. Patarin (Institut de Science des Matériaux de Mulhouse UMR CNRS 7228, France). Na-ZSM-5 and NH_4-ZSM-5 (i.e. M-MFI, M = Na^+, NH_4^+) samples (Si/Al = 13.5; average particle size ~1 µm) were obtained from VAW aluminium (Schwandorf, Germany). 3-hydroxyflavone (3HF, $C_{15}H_{10}O_3$) was obtained from Sigma. Pure and dry Ar gas was used.

2. Exchanged zeolites. To prepare Zn-ZSM-5, the initial ammonium extra framework cation of aluminated zeolites was exchanged by Zn^{2+} using the corresponding $ZnCl_2$ chloride salts (100 mL, 0.1 mol.L^{-1}). Primarily, the exchange process is carried out by suspending zeolite powder in $ZnCl_2$ aqueous solution under stirring. After 24 h, the solid phase is filtered off and dried at 200°C in an oven for 12 h, then stirred again with a fresh solution of chloride salt and then dried. The procedure is repeated 4 times. The resulting solid is washed by deionized water, isolated, dried at 200°C for 12 h and then calcined at 450 °C in ambient air for 6 h. The elementary analyses of the exchanged zeolite indicate that the ammonium cations of as-provided zeolites have been completely exchanged by Zn^{2+} using the above procedure. To get the acidic H-ZSM-5 zeolite, the NH_4^+ counterbalancing cations of the aluminated NH_4-ZSM-5 were completely converted to H^+ cations by calcination procedure in flowing air by increasing the temperature up to 450°C and holding for 6 h. The unit cell analyses of M_n-MFI correspond to $(SiO_2)_{96}$ (silicalite-1), $M_{6.6}(AlO_2)_{6.6}(SiO_2)_{89.4}$ (M= H^+, Na^+) and $Zn_{3.4}(AlO_2)_{6.6}(SiO_2)_{89.4}$. The chemical analyses, powder XRD patterns, ^{29}Si, ^{27}Al MAS-NMR,

IR, Raman, and DRUVv spectra of bare exchanged zeolites were found to be characteristic of well-crystallized porous compounds with very low amounts of extraframework aluminium species.

3. 3HF loaded zeolites. Weighed amounts (~ 1.4 g) of exchanged zeolite samples are introduced into an evacuable, heatable silica cell placed in a vertical oven connected to a piping network. The sample is heated stepwise up to 450°C under flowing dry Ar for 12 h. Then, the sample is cooled to room temperature under dry argon. Weighed amounts of 3HF corresponding to 0.5 3HF molecule per unit cell (UC) in M-MFI are introduced into the cell under dry Ar at room temperature and then the powder mixture is shaken. After homogeneous mixing, the powder is transferred under dry argon in a quartz glass Suprasil cell and sealed. All the samples are stocked in sealed cells at 40 °C for 6 months in the dark.

4. Molecular Modeling (MM). The modelling of 3HF sorption in medium pore M-MFI was performed using Material Studio Modelling package (version 5.2) from Accelrys International. The atomic positions for the zeolite frameworks were obtained from previous X-ray and neutron diffraction determinations of the structures. [25,26] In Al-containing ZSM-5, Si atoms have been substituted by Al atoms in the close proximity of Cs^+ extra framework cations whose location was determined by XRD experiments applied on Cs-exchanged ZSM-5 zeolite. [27,28] Then, the locations of extra-framework cations were optimized using Monte Carlo simulations and kept fixed during sorption modelling. The structural parameters and set of partial charges of 3HF are obtained from calculation using Atoms-in-molecules (AIM) method. [29] Monte Carlo simulations and subsequent energy minimization calculations were detailed in previous works. [30]

5. Instrumentation

5.1. Diffuse Reflectance UV-visible (DRUVv) Absorption Spectroscopy. The UV-visible absorption spectra of the samples in the ground state or after irradiation were recorded between 200 and 900 nm using a Cary 6000 spectrometer. The instrument was equipped with an integrating sphere to study the powdered zeolite samples stocked under argon in quartz cells via diffuse reflectance; the corresponding bare zeolite was used as the reference. The DRUVv spectra were plotted as the Kubelka-Munk function:

$$F(R) = (1-R)^2/2R = K/S \qquad (1)$$

where *R* represents the ratio of the diffuse reflectance of the loaded zeolite to that of the dehydrated neat zeolite, *K* designates an absorption coefficient proportional to the concentration C of chromophore and *S* the scattering coefficient of the powder. *F(R)* was registered as function of λ (wavelength) at several *t* (time).

5.2. Raman Spectrometry. A Bruker RFS 100/S instrument was used as a near-IR FT-Raman spectrometer with a CW Nd:YAG laser at 1064 nm as excitation source. A laser power of 10-100 mW was used. The spectra (4000-150 cm^{-1}) were recorded with a resolution of 2 cm^{-1} using 1200 scans.

5.3. DRIFTS. The FTIR spectrometer was a Thermo-Nicolet Magna 860 Instrument equipped with liquid nitrogen cooled MCT detector. The DRIFT spectra were recorded with 2 cm^{-1} resolution. The key part of the *in situ* DRIFTS apparatus is a Harrick Scientific Diffuse reflectance attachment "Praying Mantis" combined with cell equipped with CaF_2 windows and operating to 700 K under controlled atmosphere. The DRIFTS spectra were plotted as the Kubelka-Munk function.

5.4. 3D fluorescence emission spectroscopy. The experiments were carried out on a Fluorolog (Jobin Yvon) spectrometer using a xenon lamp (450 W) as excitation source and slit width varying from 2 to 4 nm. Three-dimensional spectra were acquired to obtain excitation-emission matrix (EEM) plots, where the excitation wavelengths are plotted on the y-axis, the emission wavelengths on the x-axis and the third dimension represents the relative intensity.

5.5. Time-Resolved Diffuse Reflectance (TRDRUVv) Absorption Spectroscopy. The experimental set-up for nanosecond diffuse reflectance spectroscopy, applicable to the detection of transient species in light-scattering systems, is analogous to that previously described elsewhere. [31,32] Excitation pulses at 355 nm (7-8 ns, 1.5 mJ) were provided by a 20-Hz Nd:YAG laser (DIVA II, Thales laser). The probe light was provided by a Xe lamp (XBO 150W/CR OFR, OSRAM). A UV filter was used to avoid photochemical reactions by the analysing light. The reflected light was dispersed by a monochromator (Horiba Jobin-Yvon, iHR320) and analysed with a photomultiplier (R1477-06, Hamamatsu) coupled to a digital oscilloscope (LeCroy 454, 500 MHz). The excitation pulse was at 90° with respect to the monochromator/photomultiplier whereas the white probe light was at a 63° angle to the detector which collected the diffuse reflected light. In the case of powder samples, the transient absorption intensity is displayed as percentage absorption (% absorption), given by % absorption=$100\times(1-R/R_0)$, where $R(\lambda,t)$ and $R_0(\lambda, t)$ represent the intensity of the diffuse

reflected white-light probe with and without excitation, respectively. Kinetic traces from 10 ns to 800 ms were detected from 430-800 nm every 5 nm from which transient spectra were reconstructed. The total instrument response time is a few tens of nanoseconds. To ensure that fresh sample is excited with each laser pulse, excitation was done at 0.3 Hz. Indeed to maintain sample integrity during the experiment, the sample was also moved and/or shaken throughout to ensure that a fresh region of the sample was probed by each laser pulse.

Nitrogen adsorption–desorption isotherms. The experiments were performed at -196°C using the ASAP2000 gas sorption system from Micromeritics in order to determine the textural properties. Before analysis, the 3HF@HZSM-5 sample was outgassed at 50 °C for 5 h under secondary vacuum in order to keep the 3HF inside microporosity (the parent material was outgassed at 250°C). The BET model was used to calculate the surface area of the samples for relative pressures between 0.01 to 0.30. The different porous volumes (microporous and mesoporous) were determined from αs-plots using the Jaroniec's non porous silica adsorption isotherm as reference. [33]

5.7. Data Processing. The kinetics were analysed through the ***C(t)*** decays. Mono or two exponentials do not reproduce accurately the decays. The concentration decay ***C(t)*** was accurately fitted using the Albery function which takes into account the non-homogeneity of the material. [34] The decay kinetic fitting was carried out by using the Microcal™ Origin software.

Results

Molecular Modeling. MM was carried out using the Monte Carlo method and subsequent energy minimization of the non-bonding interactions between 3HF and fixed zeolite framework followed by geometry optimization procedure. Calculations take into account the atom-atom interactions between zeolite and guest molecule. The MFI zeolite structure is constituted by two types of intersecting channels: the straight one with nearly circular opening (0.53 x 0.56 nm^2) and the sinusoidal one with an elliptical opening (0.51 x 0.55 nm^2). For silicalite-1, the results of the calculation show that the preferred 3HF sorption site is located in the straight channel at the intersection with the sinusoidal channel. The energy minimization leads to occluded 3HF with non-planar geometry, the dihedral angle between the chromone plane and the benzyl ring being 46°. In MZSM-5 (M= Na^+, H^+), the guest molecule is in close interaction with the charge compensating cation through the oxygen atom of the C=O double

bond (Fig. 1). The Na^+ ···· O=C distances and SiO(Al)-H ···· O=C are found to be 2.07 Å and 2.22 Å in NaZSM-5 and HZSM-5 respectively. In acid HZSM-5, the short distance between C=O of 3HF and OH group of zeolite is consistent with the formation of a possible hydrogen bond and thus, with the inhibition of the intramolecular hydrogen bond involved in the ESIPT. Non planar 3HF geometries are also obtained in both cases with dihedral angles between chromone and benzyl planes of 26 and 54° in NaZSM-5 and HZSM-5, respectively. These results and distances are in agreement with the data reported by Pahari et al. [35] for 3HF encapsulated in γ-cyclodextrin nanocavities in which hydrogen bond was assumed to be formed between the non-planar guest and the host. In the case of ZnZSM-5 zeolite, as the modelling is only based on van der Waals and coulombic interactions, the partially covalent bond character expected between 3HF and Zn^{2+} cation cannot be considered. Consequently, the results of molecular modelling are not taken into account for this sample. Thus, molecular modelling calculations predict the possibility of 3HF molecule to find preferential sorption sites in the channel even if the molecule dimensions were assumed to be slightly larger than the channel size. Thus, the flexibility of the molecule and the deformation of the crystal lattice have to be considered to allow 3HF penetration into the zeolite void space. This point was initially emphasized by Derouane in its description of the confinement effect in zeolites and of their behaviour as solid solvents when the size of the guest molecule and of the channels or cages are comparable. [36] Indeed, to maximize their van der Waals interactions, the guest and the host framework may reciprocally optimize their respective structures. To this aim, molecules can contract to penetrate into pores with size (down to about 80%) smaller than their free (gas phase) molecular size and the zeolite framework can be distorted at least locally upon adsorption considering the magnitude of the physical interactions which are involved. [37] In addition, it is important to note that atoms of the lattice and of the adsorbed molecules are vibrating. This allows also diffusion of molecules through the windows and pores, even if the dimensions of the molecule are somewhat larger than those of the windows/pores.

Sorption isotherms. The isotherms are of Type I (IUPAC classification) as exemplified in Fig. 2 for HZSM-5 zeolite samples. From the textural characteristics derived from these curves (Table 1), a decrease of the microporous volume and surface area is observed for sample 3HF@HZSM-5, which provides evidence of the incorporation of 3HF within the internal volume of the zeolite framework. This decrease is quite slight since the number of adsorbed molecule is relatively low (0.5 3HF /UC, theoretically). The result obtained for 3HF@HZSM-5 is supposed to be representative of the behaviour of all the samples.

Spectral investigation of 3HF sorption in silicalite-1 and in MZSM-5 (M=Na^+, H^+, Zn^{2+}). After mixing dry solid 3HF and dehydrated zeolite, the sample evolution was followed as a function of time using complementary optical spectroscopy techniques. The spectral development monitored by DRUVv, Raman scattering and FT-IR absorption appeared to be complete after 3 months in silicalite-1 and after 6 months in MZSM-5 (M = Na^+, H^+, Zn^{2+}). The corresponding reaction mechanism can be denoted as follows: 3HF + MFI → 3HF@MFI with MFI = silicalite-1 or MZSM-5 where (M = H^+, Na^+, Zn^{2+}) and 3HF@MFI corresponds to the 3HF molecule adsorbed on or within the zeolite framework. After completion, the 3HF@silicalite-1 sample kept in the dark remained white whereas the mixing of 3HF white powder with dehydrated MZSM-5 (M=Na^+, H^+, Zn^{2+}) generated light yellow powders under identical experimental conditions.

Due to the close match between 3HF size and pore diameters as deduced from the results of molecular modelling, strong interactions are expected between the guest molecule and the framework. These interactions which depend on the presence of extra framework cation M^+ can modify significantly the spectral features of 3HF in its sorption site. Thus, the spectral data for 3HF adsorbed in MFI are presented below by zeolite type. DRUVv, Raman scattering, infrared absorption, fluorescence emission and TRDRUVv are used to characterize ground and excited states.

Silicalite-1. The DRUVv spectra show essentially a broad band at 325 nm with maxima centred at 305 and 345 nm (Fig. 3b). These spectral features are very similar to the UV-vis spectrum of 3HF recorded in solid phase and characteristic of the normal form of 3HF, (Fig. 3a). [12]

The FT-Raman and IR spectra recorded for 3HF occluded in silicalite-1 are presented in Fig. 4b and 5b in comparison with the vibrational spectra of solid 3HF (Fig. 4 and 5, spectrum a). The Raman spectrum of 3HF@silicalite-1 remains identical to that of solid 3HF in terms of position and of relative intensities from mixing to several months and even years. Note that the contributions of the silicalite-1 framework are very weak in the Raman spectra. In the infrared spectrum, the vibrational modes of pure silicalite-1 are huge and overlap drastically the infrared spectrum of 3HF@silicalite-1 especially below 1300 cm^{-1}. Nevertheless, most of the lines observed for 3HF@silicalite-1 sample between 1350 and 1600 cm^{-1} are similar to those observed for solid 3HF and show the same positions and relative intensities. This points out the fact that 3HF does not undergo significant interaction upon sorption within silicalite-1.

The 3D fluorescence emission spectra of 3HF incorporated in silicalite-1 display emission band centred at 530 nm upon excitation at 350 nm (Fig. 6b). This technique which provides information on the electronic excited state indicates that tautomer T* form is favored at the excited state as reported in apolar and aprotic environments [38-42]. By comparison, the fluorescence spectrum obtained for solid 3HF displays clearly two emission maxima at 530 nm and at 470 nm corresponding to the T* and N* [23] forms, respectively (Fig. 6a). Unlike silicalite-1, the observation of the N* form in addition to the tautomer form is probably due to strong interaction between molecules in the solid state. In contrast, within silicalite-1 molecules are assumed to be isolated without any interaction between each other's because of low loading rate and then, no interaction with polar environment can occur. This feature confirms the incorporation of the molecule within the channel of silicalite-1. Sorption on the external surface would probably lead to many monolayers in which molecules are in close interaction. In such case, the fluorescence spectrum would be analogous to that observed with solid 3HF. To get further information, time resolved DRUVv experiments were carried out to investigate the electronic excited state by using exciting lines at 320, 355 and 410 nm. Only the 355 nm exciting line allowed the observation of poorly resolved bands maximizing between 460 and 490 nm (not shown). According to the data reported in the literature which were obtained in various solvents, absorption bands ranging between 460 and 480 nm might be assigned to the T* form [38-42]. However in the present case, the calculation of the lifetimes using the Albery method applied on the decays recorded for the bands observed at 460 and 475 nm seems to indicate the presence of different transient species with lifetimes ranging between 35 μs ($k = 0.0287\ \mu s^{-1}$) at 475 nm and 490 μs ($k = 0.00205 \mu s^{-1}$) at 460 nm. Due to the weak intensity of the spectra recorded between 5 and 500 μs, no clear assignment can be done.

NaZSM-5. The DRUVv spectra recorded for 3HF@NaZSM-5 6 months after the mixing display a very broad band between 250 and 450 nm including 2 main contributions centered at 315 nm and at ca. 400-410 nm with 2 shoulders at 400 and 435 nm (Fig. 3c). The 315 nm band is more intense and is assigned to the N form [12] whereas no obvious attribution can be proposed for the 400-410 nm band which does not correspond to any known species at the ground state. The assignment is discussed below in the discussion section.

The Raman spectrum is identical to that of solid 3HF and is characteristic of 3HF molecule (Fig. 4). It does not show any features characteristic of possible perturbation due to the environment. Using FT-IR spectroscopy, the spectrum is also highly perturbed below 1200

cm^{-1} due to strong overlapping with the vibrational modes of pure NaZSM-5 (Fig. 5, spectrum c). Thus, comparison is made for the 1250-1750 cm^{-1} spectral range for solid 3HF, 3HF@silicalite-1 and 3HF@NaZSM-5. The main differences between 3HF in the solid phase or in silicalite-1 and 3HF@NaZSM-5 are due to changes of relative intensity. The changes observed in the spectra are probably due to the perturbation induced by the presence of the cation which induces a change of the polarization in the molecule environment.

The 3D fluorescence emission spectra show 2 bands centred at 535 with excitation at 362 nm and 470 nm with excitation at 300 nm (Fig. 6c). The 535 nm band is assigned to T* whereas the 470 nm one corresponds to the N* form [14,18,23].

The TRDRUVv experiments show 2 absorption bands at 470-480 nm and at 530 nm when using an exciting line at 355 nm (Fig. 7A). These 2 bands come probably from two different excited species as shown by their corresponding lifetimes deduced from the Albery model applied on the normalized kinetic trace for the decays (Fig. 7B). The lifetimes are 165 µs ($k = 0.00205\ \mu s^{-1}$) and 746 µs ($k = 0.00134\ \mu s^{-1}$) for the species associated with the bands at 470-480 nm and at 530 nm, respectively. As discussed for silicalite-1, most of the previous studies have reported that the 470-480 nm band correspond to the T* form of 3HF. The 530 nm band is much less documented but might be assigned to the N* form [43].

HZSM-5. Fig. 3d shows the DRUVv spectrum obtained 8 months after mixing 3HF and HZSM-5. The spectrum displays two bands at about 400 nm with high intensity, the origin of which being still unclear (see discussion section) and at ca. 320 nm with medium intensity assigned to the normal form (N) of 3HF. The Raman spectrum is still characteristic of 3HF molecule and does not allow distinguishing between the normal and hypothetic other 3HF forms (Fig. 4). The IR spectrum is similar to that recorded for 3HF@NaZSM5 but shows a little more differences in terms of relative intensity compared with the spectrum recorded for 3HF in silicalite-1 (Fig. 5, spectrum d). Unfortunately, no obvious evidence allows us to assign these differences to any particular 3HF form and to explain these features, it is more reasonable to consider the change of the internal electrostatic field when going from the silicalite-1 to HZSM-5. A weak new band is observed at 1326 cm^{-1} but due to the poor signal/noise ratio, no reasonable assignment could be performed. Nevertheless, note that two weak bands at 1685 and 1705 cm^{-1} are observed after sorption of 3HF in HZSM-5 whereas the 1705 is very weak for solid 3HF and for 3HF occluded in silicalite-1 and the 1685 cm^{-1} band is not observed with silicalite-1 and in NaZSM-5. These changes might indicate perturbation in the proximity of the C=O bond.

The emission spectra show essentially a band at 455 nm with excitation at 305 nm (Fig. 6d). This band is tentatively assigned to the N* form by analogy with the 470 nm observed in NaZSM-5 and reported in the literature. [14,18,23]

The TRDRUVv experiments carried out after 3HF sorption in HZSM-5 were not successful and only a very weak band at 475 nm was observed with very low signal/noise ratio using the 355 nm exciting line.

ZnZSM-5. The DRUVv spectrum shows a broad band extending between 300 and 475 nm with two maxima at 320 and 400 nm which are assigned to the complexed form of 3HF with Zn^{2+} cation [8,9] (Fig. 3e). The Raman spectrum exhibits significant changes compared to those obtained for solid 3HF and for 3HF occluded within Na^{+} and HZSM-5 (Fig. 4B, spectrum e). New lines are observed at 1520, 1465, 1419, 1323, and 1232 cm^{-1} and relative intensity changes are also noticeable for instance for I(991)/I(997) and for I(1595)/I(1616). In such complex, the modification of the bond lengths upon participation of mesomeric forms in the chelate structure is expected to induce frequency variation and was often reported in the presence of metal cations like Al^{3+},[6,10,19] Pb^{2+} and Zn^{2+} [7]. Thus, the appearance of the 1520 cm^{-1} and 1465 cm^{-1} bands are assumed to be due to the decrease of the C=O bond order upon chelation with Zn^{2+} cation. Even if the C=O and C-O bond lengths are not really identical, the corresponding stretching modes are probably mechanically coupled in a symmetric and an asymmetric ways. Particularly, the 1520 cm^{-1} line is assigned to the asymmetric stretching mode whereas the 1465 cm^{-1} line corresponds to the symmetric stretching mode.

The IR spectrum is poorly resolved and very few bands are observed below 1300 cm^{-1}. Above 1300 cm^{-1} (Fig. 5 A and B, spectrum e), some lines also observed for solid 3HF at 1309, 1321, 1353 cm^{-1} are still present for 3HF@ZnZSM-5 but the assignment of these contributions in ZnZSM-5 sample are difficult since these modes of vibration involve several groups. [44-47] However, it should be noted that some intense lines of 3HF usually observed at 1473 (phenyl ring + CH i.p. bending + OH bending), 1484 and 1492 cm^{-1} involving particularly the benzo ring in the chromone system and 1567 cm^{-1} (benzo ring in the chromone system, C=O stretching, OH bending) are not observed anymore upon sorption within ZnZSM-5. In contrast, two new bands are observed at 1487 and 1558 cm^{-1} and a shoulder at 1465 cm^{-1}. These lines might again correspond to the vibrational contribution to the benzo ring in the chromone system but probably do not involve anymore the OH bending due to the assumed 3HF chelation with Zn^{2+} cation.

The emission spectra display a broad band that extends between 460 and 510 nm maximizing at 480 nm (Fig. 6e) which is assigned to the metallic $Zn(3HF)^+$ complex in agreement with the spectrum reported in methanol solution observed at 475 nm [7]. This result confirms the data obtained by DRUVv absorption and Raman scattering.

The TRDRUVv spectra obtained using exciting lines at 355 nm are presented in Fig. 8A. The spectra show one intense band centred at 470 nm and one weak band at 510 nm. The normalized kinetic traces for the decay of the transient species observed at 470 nm (Fig. 8B) and at 510 nm (not shown) following laser excitation of 3HF@ZnZSM-5 are accurately simulated according to the heterogeneous Albery kinetic model. The corresponding lifetimes are 45 μs (k= 0.02235 μs^{-1}) and 42 μs (k=0.02368 μs^{-1}), respectively. These lifetimes are found to be very similar and it might indicate that the two bands correspond to the same species corresponding to the excited complex.

Discussion

Molecular modelling shows the possibility of 3HF molecule to pass through the pore entry and to diffuse to preferred sorption site. The 3HF incorporation into the internal volume is confirmed by the decrease of the microporous volume observed by nitrogen adsorption-desorption isotherm measurements. Then, in addition to modelling and porosity measurements, vibrational spectroscopy provides information of the 3HF ground state after mixing. For silicalite-1, the Raman and infrared spectra are very similar to that of solid 3HF. This result shows that molecule is occluded as an intact molecule in the zeolite channel and can be considered to be in an isolated state. Within NaZSM-5 and HZSM-5, 3HF molecules undergo probably interaction with the charge compensating cations and thus, the modifications of the local electrostatic field around the guest induce some perturbations on the vibrational modes. No clear assignment of possible different 3HF forms could be proposed with these data. These results may indicate non-significant change in 3HF geometry (symmetry group) upon sorption. In contrast, after mixing with ZnZSM-5, chelation of 3HF with Zn^{2+} is clearly identified on the Raman spectrum. Thus, the different spectral features observed using Raman and IR spectroscopies probably indicate that the 3HF molecules can penetrate into the channels of silicalite-1, MZSM-5 (M = H^+, Na^+, Zn^{2+}) zeolites. This hypothesis is also coherent with the fact that external surface area sites are just a very small fraction of the overall adsorption capacity. Note that even if the fit is very tight, ortho-xylene with comparable steric effect was already found to diffuse very slowly in HZSM-5. [48,49]

However, this hypothesis has to be confirmed by using absorption and emission spectra. As zeolites can be considered like solid solvents, different behaviours are expected upon guest incorporation into the host framework because the spectral features for both the normal, tautomer and complex forms are assumed to be modulated by H-bonding, polarity and related effects. The solvent effect was already intensively studied in many solvents to determine how 3HF behaves in the presence of aprotic or protic, and/or polar or apolar surrounding media. All these works show that the tautomeric equilibrium is very dependent on the protic nature and polarity of the 3HF molecule environment. In apolar and aprotic solvent like n-heptane, the proton transfer is favoured at the excited state whereas in highly polar solvent, like methanol, the normal form is still observed in addition to the tautomer form. Competition between intramolecular and intermolecular proton transfers is put forward to explain these results since intermolecular hydrogen bonds can inhibit the formation of the tautomeric form. [4,12,13,21,50] If most of the studies undertaken to investigate the photochemical behaviour of 3HF were performed in solution using different types of solvents, some works were also carried out to investigate the behaviour of 3HF under confinement upon incorporation in various host materials. 3-HF was adsorbed in media like γ- or β-cyclodextrins [17,35] and sol gel glass matrices [18,19]. Only one group reported the sorption of 3HF into zeolite nanoparticles in colloidal suspension [23]. So far, the incorporation of 3HF into zeolite nanocrystals or microcrystals without any solvent was never investigated. The hydrophobic internal environment in the cyclodextrin nanocavities was found to reduce significantly the solvent mediated perturbations, such as external hydrogen bonding. Thus, the minimization of this competitive process makes easier the formation of intramolecular H-bond associated with the ESIPT process. Consequently, the inclusion of 3HF in such environment leads to a huge tautomer emission compared to what is observed in aqueous buffer. Note that the polarity in a cyclodextrin cavity was found to be similar to that of alcoholic solvent. [35] In addition, it was demonstrated that the intensity of the T* form is also significantly enhanced in cyclodextrin with higher confinement where the average environment of the entrapped 3HF is more hydrophobic. In sol gel glass matrix, strong solvatochromic effects were also reported with the presence of high intensity T* fluorescence band around 515 nm and the absence of signal around 410 nm, as expected for the N* form. These findings highlight that the chemical environment of 3HF within these matrices consists of low polarity functional groups. Furthermore, the perturbation of the N and T forms energy levels showed that the rigidity of the surrounding framework can play a significant role in the deactivation of the excited states. [18] In contrast, the 3HF incorporation in beta type zeolite suspension in ethanol showed that the

N* form was clearly favoured compared to pure ethanol in which dual emission was observed with the presence of both N* and T* forms [23]. In beta zeolite, the modification of the emission spectrum clearly showed that intermolecular hydrogen bonds were created and that the intramolecular proton transfer leading to the tautomeric form was inhibited. Based on the data of the literature concerning solvent effects, the environment within the cavities of this beta zeolite in colloidal suspension was assumed to be much more polar than in ethanol taken as reference. Thus, the interpretation of the results obtained after mixing 3HF and MFI type zeolites without any solvent is based on the data previously obtained in solution for various solvents and under confinement using different matrices to encapsulate the guest molecule.
Depending on the presence of charge compensating cation and on its nature, the sorption of 3HF induces dramatic changes in the emission and absorption behaviours of 3HF, the zeolite being effectively considered as a solid solvent. [51] Afterwards, the data obtained for 3HF occluded within zeolite channels are compared to 3HF bulk state. The DRUVv spectrum of bulk 3HF shows a narrow band centred at 225 nm and a broad band extending between 300 and 400 nm. The EEM fluorescence exhibits particular features: for excitation wavelengths lower than 420 nm, an emission is observed at ca. 530 nm characteristic of the tautomer form emission; for higher excitation wavelengths (lower energies), only the N* fluorescence is detected at 470 nm. Note that dual fluorescence (for a given excitation wavelength) is never observed. To explain these phenomena, it is well known that the stacking effect existing in solid state between 3HF molecules favours the intramolecular hydrogen bonds and thus the formation of the tautomer in the excited state. [52] However, by exciting in the absorption band foot (above 420 nm), the energy is not sufficient enough to cross the energy barrier between the N* and T* forms and then only the N* fluorescence is observed.

Within the purely siliceous microporous volume of silicalite-1, the apolar and hydrophobic environment hinder all mediated perturbations and allows the formation of intramolecular H bond as observed in the ESIPT mechanism leading to the T* form. This is consistent with previous studies carried out using various apolar and aprotic solvents or cyclodextrins as described above. In contrast, in the acidic HZSM-5, the 3HF molecules are assumed to be occluded in the proximity of the charge compensating H atoms which can induce significant perturbations through hydrogen bonding interfering with the intrinsic ESIPT. The tautomer emission is known to be highly sensitive to external hydrogen bonding perturbation since this process can compete with the intramolecular H-bond formation related to the tautomerization. Moreover, it should be noted that the polar character of the environment is also significantly

enhanced by the presence of protons. The high polarity leads to an increase of the energy barrier height between the normal and the tautomer form in the excited state. Then, as the emission spectra in HZSM-5 display exclusively a fluorescence band at 455 nm probably characteristic of the N* form, it can be deduced that the tautomer formation is totally inhibited [17]. Note that intermolecular H-bonds are assumed to not occur in HZSM-5 since the preparation mode of the sample should leads to 0.5 molecules per unit cell to avoid any contact between molecules.

Upon sorption within NaZSM-5 channels, the 3D fluorescence spectra show the spectral features of both the normal and the tautomer forms. The EE matrix shows emission wavelengths identical to those obtained for solid 3HF. This sample exhibits an intermediate behaviour between what is observed in the silicalite-1 and in the HZSM-5. These data might be explained by the chemical surrounding of the 3HF molecule which is constituted by Na^+ extraframework cations and –(Si-O-Al)– groups which induce more polar conditions in NaZSM-5 zeolite than in silicalite-1 where T* formation is favoured and less polar than in HZSM-5 (where proton leads to higher electric field gradient than Na^+) in which N* is assumed to be stabilized as unique excited species.

In addition, it is interesting to note that if the polar hydroxyl groups Si-O(H)-Al correspond to Brønsted acid sites, there also exists non-acidic Si-O(H)-Si silanol groups which are necessary to terminate the external surface of the zeolite crystals. Internal silanol groups are also present at structural local defects or at missing T-atoms (T = Si, Al). However, these silanols are known to be not involved in reactivity as reported in numerous papers dealing with heterogeneous catalysis. The surrounding of this group is not favorable enough to allow easy proton transfer to the adsorbed molecules. The case of silicalite-1 is particularly striking as this apolar and aprotic medium hinders all mediated perturbations and leads readily to the formation of intramolecular H bond.

It is worth noting that the fluorescence emission in the present zeolite samples depends on the absorption band implied in the excitation. When high energy excited states are involved, the N* fluorescence is observed. In contrast, the low energy states give rise to the T* fluorescence.

In addition, it is interesting to note that the Stokes shifts deduced from excitation/emission spectra for T* in silicalite-1 (λex= 350 nm; λem= 530 nm: $\Delta\lambda$=180 nm) and in NaZSM-5 (λex= 362 nm; λem= 535 nm: $\Delta\lambda$=173 nm) show a good agreement with the data reported in the literature for various solvents like water (λex= 341.4 nm; λem= 508 nm: $\Delta\lambda$=166 nm) or

β-cyclodextrin (λex= 341.7 nm; λem= 521.5 nm: Δλ=179 nm). [17] and with solid 3HF (λex= 400 nm; λem= 530 nm: Δλ=130 nm). These similar values seem to show that the T* Stokes shift remains nearly constant whatever the solvent or the matrix is and thus, provide evidence of the assignment of the fluorescence emission observed in the MFI samples.

In contrast, the Stokes shift corresponding to the N* form is not found to be in the same order in both HZSM-5 (λex= 305 nm; λem= 455 nm: Δλ= 150 nm) and NaZSM-5 (λex= 300 nm, λem= 470 nm: Δλ= 170 nm) compared to β-cyclodextrin (λex= 341.7 nm; λem= 406.5 nm: Δλ=64,8 nm), water (λex= 341.4 nm; λem= 409 nm: Δλ= 67.6 nm) [17], 3HF loaded zeolite beta suspension (λex= 397 nm; λem=444 nm: Δλ=47 nm), ethanol (λex= 367 nm; λem= 415 nm: Δλ=48 nm) [23] and even solid 3HF (λex=430 nm; λem= 470 nm: Δλ= 40 nm). The difference between the Stokes shift values obtained using the present EEM spectra and the data reported in the literature might be explained by the fact that the N* fluorescence is observed only when high energy excited states are implied in the excitation. Consequently, the excitation wavelength giving rise to the maximum of fluorescence emission obtained using the EEM is different from the λmax of absorption recorded by DRUVv. This phenomenon seems to be characteristic of MFI zeolites and can be explained by the confinement within the internal space of these microporous materials which can induce significant modifications of the potential surfaces of excited states and their intersections.

The DRUVv spectra recorded for 3HF adsorbed in silicalite-1, NaZSM-5 and HZSM-5 show all a broad band extending between 250 and 450 nm with two maxima peaking at ca. 320 nm and at about 400 nm. However, significant differences can be noticed between silicalite-1 for which the spectrum displays essentially a contribution centred at 320 nm and HZSM-5. Indeed, the spectrum of 3HF occluded in HZSM-5 shows a main band at 400 nm in addition to that observed at 320 nm with medium intensity. NaZSM-5 which corresponds to a moderately polar environment leads to an intermediary state with both forms. The 320 nm band which is clearly stabilized in apolar and aprotic silicalite-1 corresponds to that reported in literature and assigned to the 3HF normal form. [12]. In contrast, in the present study, no clear evidence based on previous works could be proposed to assign the 400 nm band observed in the highly polar and protic HZSM-5 internal structure. The presence of an absorption band between 400 and 450 nm was already reported for 3HF encapsulated in γ-cyclodextrin [16] and in protic solvent like methanol. [12,15] In cyclodextrin, the increase of absorption band at 420 nm was attributed to the formation of an inclusion complex between 3HF and the cyclodextrin due to the migration of a proton from the encapsulated 3HF to the framework. Similarly, in

methanol, the 410 nm absorption was assigned to the 3HF anionic form. Nevertheless, these acido-basic reactions can occur only if the 3HF behaves as an acid to give a proton. For cyclodextrin, the ground state 3HF acidity is effectively known to be increased upon incorporation [16] whereas with methanol, the aromatic hydroxyl compounds are generally stronger acids compared to aliphatic hydroxyl compounds and then alcohol can abstract a proton from 3HF. [12] Unfortunately, this reaction mechanism cannot be put forward to explain the spectrum obtained with HZSM-5 because of the very high acidity within the channels of this zeolite as determined using 2,2'-and 4,4'-bipyridine probe molecules. [53]

To explain this 400 nm band, we might also put forward the results of Stradjord [4] who showed that the absorption spectrum of the normal form is shifted toward lower energy when 3HF is hydrogen bonded to the solvent. The very high polar and protic environment within HZSM-5 channels might induce such red shift.

The assignment of the 400 nm band to a stable tautomer form cannot also be directly ruled out. The formation of this T form was only reported to be obtained from the photoexcitation of the N form followed by relaxation to T* excited state. Techniques such as transient absorption and/or stimulated emission pumping have evidenced a band around 400 nm assigned to a transition involving T and T* states. Nevertheless, the lifetime of the T ground state was found to be in the μs range. This low lifetime is due to the fast reverse proton transfer toward the N form. [38] To explain the possible presence of stable tautomer ground state in HZSM-5, one might also consider that the treatment of motion along the solvent polarization coordinate is comparable to that developed in electron transfer theories. [54] This model was proposed previously by Kelley to explain how the presence of hydrogen bonding environment and the polarization can inhibit the intramolecular hydrogen bond by drastically decreasing the ESIPT rates. The energetic barriers are indeed modulated by the solvent and consequently, the proton transfer dynamics is largely controlled by the nature and properties of the solvent. [50] Even if this model was only applied to investigate the proton transfers at the excited state, one can wonder whether these solvent-induced barriers can be modified for the ground state leading to tautomer stabilization in HZSM-5. Note also that in the case of 3HF@HZSM-5, the 400 nm is observed using conventional spectroscopy and is associated with a stable state. However, even if the particular host composition might induce such T ground state stabilization, no obvious spectral features are observed using Raman and IR spectroscopy to highlight this hypothesis. Indeed, formation of such stable ground state tautomer form would lead to significant changes on the vibrational spectra, especially for C=O and C-OH bands. The absence of marked modifications when passing from silicalite-1

to HZSM-5 is not compatible with ground state tautomer formation in the acid HZSM-5 zeolite and thus, this hypothesis has to be discarded. Consequently, in the light of all the assumptions discussed above, no clear assignment can be proposed for the 400 nm band and further work is required to establish the origin of this band.

In the presence of metal Zn(II)-containing solution, chelation of metal is known to take place at the level of the α-hydroxyl-carbonyl group with a total deprotonation of the hydroxyl. [7] Even if the chelating power of Zn(II) is not very efficient compared to Al(III), large absorption and emission bands were observed at ca. 410 nm and 475 nm, respectively. In the case of 3HF adsorbed in ZnZSM-5, the present results show analogous but strong features characteristic of the formation of the metal complex within the zeolite channel. In addition, the Raman spectra confirm these results by the observation of a significant shift of the line assigned to the C=O bond due to the reduction of the bond order.
It is interesting to note that no contribution of remaining isolated 3HF molecule is observed on the fluorescence emission spectra. These findings demonstrate the presence of the molecule within the ZnZSM-5 channel and point out the strong interaction between the metal cation and the guest molecule.

Conclusion

The totally different behaviours observed in dealuminated silicalite-1 and Al-rich ZSM-5 containing H^+, Na^+ or Zn^{2+} using complementary optical spectroscopies show evidence of the strong interaction between charge compensating cations and 3HF molecules. This zeolite-depending reactivity compared to 3HF in the solid phase or in various solvents clearly shows the incorporation of the dye molecule within the internal void space since the charge compensating cations are assumed to be located essentially in the internal volume. These spectral data confirm the porosity measurements and firmly support the molecular modelling calculations which predict the possibility of 3HF molecule to find preferential sorption sites in the channel even if the molecules dimensions were assumed to be slightly larger than the channel size. Thus, the flexibility of the molecule and the lattice deformation have to be considered to allow 3HF penetration into the zeolite void space.

In silicalite-1, 3HF is incorporated in non-polar and non-protic environment and does not seem to undergo any interaction with the channel walls. Consequently, upon excitation,

the molecule considered as isolated show easy tautomer formation. In contrast, after sorption in HZSM-5, 3HF is in close interaction with the acid proton of zeolite which inhibits the intramolecular proton transfer leading to the observation of only normal form at the excited state. For NaZSM-5, the spectral data show again an intermediary behaviour due to aprotic but polar environment, in agreement with 3HF sorption in close proximity to the Na^+ extraframework cation. Finally in ZnZSM-5, 3HF displays the same spectral features as those reported upon metallic complexation that confirm the formation of $Zn(3HF)^+$.

These results are in total agreement with the data previously reported for various surrounding media and provide information on the nature of the guest internal microenvironment, the zeolite being considered as a solid solvent.

References

1. J.B. Harborne and C.A. Williams, *Phytochem*., 2000, **55**, 481-504.

2. C. Rice-Evans, *Curr.Med.Chem*, 2011, **8**, 797-807.

3. P.K. Sengupta and M. Kasha, *Chem. Phys. Lett*., 1979, **68**, 382-385.

4. A.J.G. Strandjord and P.F. Barbara, *J. Phys. Chem.*, 1985, **89**, 2355-2361.

5. Y.A. Davila, M.I. Sancho, M.C. Almandoz and S.E. Blanco, *Spectrochim. Acta A*, 2012, **95**, 1-7.

6. T. Doussineau, D. Berthomieu, N. Floquet and M. Smaïhi, *J. Phys. Chem. C*, 2007, **111**, 7578-7585.

7. S. Protti, A. Mezzetti, C. Lapouge and J.P. Cornard, *Photochem. Photobiol. Sci.*, 2008, **7**, 109-119.

8. J.P. Cornard, L. Dangleterre and C. Lapouge, *Chem. Phys. Lett.*, 2006, **419**, 304-308.

9. C. Lapouge, L. Dangleterre and J.P. Cornard, *J. Phys. Chem. A*, 2006, **110**, 12494-12500.

10. A.C. Boudet, J.P. Cornard and J.C. Merlin, *Spectrochim. Acta A*, 2000, **56**, 829-839.

11. M.Y. Moridani, J. Pourahmad, H. Bui, A. Siraki and P.J. O'Brien, *Free Radic. Biol. Med.*, 2003, **34**, 243-253.

12. P.K. Mandal and A. Samanta, *J. Phys. Chem. A*, 2003, **107**, 6334-6339.

13. T.C. Swinney and D.F. Kelley, *J. Phys. Chem.*, 1991, **95**, 10369-10373.

14. G.A. Bruker, T.C. Swinney and D.F. Kelley, *J. Phys. Chem.*, 1991, **95**, 3190-3195.

15. S. Mondal, S. Basu and D. Mandal, *Chem. Phys. Lett.*, 2009, **479**, 218-223.

16. L. Tormo and A. Douhal, *J. Photochem. Photobiol. A*, 2005, **173**, 358-364.

17. A. Banerjee and P.K. Sengupta, *Chem. Phys. Lett.*, 2006, **424**, 379-386.

18. S. Carturan, A. Quaranta, G. Maggioni, A. Vomiero, R. Ceccato and G. Della Mea, *J. Sol-Gel Sci. Technol.*, 2003, **26**, 931-935.

19. S. Protti, K. Raulin, O. Cristini, C. Kinowski, S. Turrell and A. Mezzetti, *J. Mol. Struc.*, 2011, **993**, 485-490.

20. M. Buffa, S. Carturan, A. Quaranta, G. Maggioni and G. Della Mea, *Optical Materials*, 2012, **34**, 1219-1224.

21. J. Guharay, R. Chaudhuri, A. Chakrabarti and P.K. Sengupta, *Spectrochim. Acta A*, 1997, **53**, 457-462.

22. T. Shyamala and A.K. Mishra, *Photochem. Photobiol.*, 2004, **80**, 309-315.

23. T. Doussineau, M. Smaïhi, S. Balme and J.-M. Janot, *ChemPhysChem*, 2006, **7**, 583-589.

24. S. Hashimoto, *J. Photochem. Photobiol C: Photochem. Rev.*, 2003, **4**, 19-49.

25. B. F. Mentzen, *J. Phys. Chem. C*, 2007, **111**, 18932-18941.

26. B. F. Mentzen, G. Bergeret, H. Emerich and H.P. Weber, *J. Phys. Chem. B*, 2006, **110**, 97-106.

27. D. H. Olson, N. Khosrovani, A. W. Peters and B. H. Toby, *J. Phys.Chem. B*, 2000, **104**, 4844-4848.

28. E. Beerdsen, D. Dubbeldam, B. Smit, T.J. Vlugt and S. Calero, *J. Phys. Chem. B*, 2003, **107**, 12088-12093.

29. R.F.W. Bader, Atoms in molecules: a quantum theory, Clarendon P; Oxford University Press, New York, 1994

30. M. Hureau, A. Moissette, K. Smirnov and H. Jobic, *J. Phys. Chem. C*, 2012, **116**, 15510-15518.

31. F. Wilkinson and C. J. Willsher, *Appl. Spectrosc.*, 1984, **38**, 897-901.

32. M. Sliwa, P. Naumov, H. Choi, Q. Nguyen, B. Debus, S. Delbaere and C. Ruckebusch, *ChemPhysChem.*, 2011, **12**, 1669−1672.

33. M. Jaroniec and M. Kruk, *Langmuir*, 1999, **15**, 5410-5413.

34. W. J. Albery, P. N. Bartlett, C. P. Wilde and J. R. Darwent, *J. Am. Chem. Soc.*, 1985, **107**, 1854–1858.

35. B. Pahari, S. Chakraborty and P.K. Sengupta, *J. Mol. Struc.*, 2001, **1006**, 483-488.

36. E.G. Derouane, *J. Mol. Catal. A*, 1998, **134**, 29-45.

37. E.L. Wu, S.L. Lawton, D.H. Olson, A.C. Rohrman and G.T. Kokotailo, *J. Phys. Chem.*, 1979, **83**, 2777-2781.

38. T.P. Dzugan, J. Schmidt and T.J. Aartsma, *Chem. Phys Lett.*, 1986, **127**, 336-342.

39. K. Chevallier, M.M.N. Wolf, A. Funk, M. Andres, M. Gerhards and R. Diller, *Phys. Chem. Chem. Phys.*, 2012, **14**, 15007-15020.

40. M. Itoh and Y. Fujiwara, *Chem. Phys. Lett.*, 1986, **130**, 365-367.

41. M. Itoh, Y. Tanimoto and K. Tokumara, *J. Am. Chem. Soc.*, 1983, **105**, 3339-3340.

42. S. Ameer-Beg, S.M. Ormson, R.G. Brown, P. Matousek, M. Towrie, E.T.J. Nibbering, P. Foggi and F.V.R. Neuwahl, *J. Phys. Chem. A*, 2001, **105**, 3709-3718.

43. C. Rulliere and A. Declemy, *Chem. Phys. Lett.*, 1987, **134**, 64-69.

44. T. Teslova, C. Corredor, R. Livingston, T. Spataru, R.L. Birke, J. Lombardi, M.V. Canamares and M. Leona, *J. Raman Spectrosc.*, 2007, **38**, 802-818.

45. M. Wang, T. Teslova, F. Xu, T. Spataru, J.R. Lombardi and R.L. Birke, *J. Phys. Chem C*, 2007, **111**, 3038-3043.

46. A. Vavra, R. Linder and K. Kleinermanns, *Chem. Phys. Lett.*, 2008, **463**, 349-352.

47. C. Corridor, T. Teslova, M. V. Canamares, Z. Chen, J. Zhang, J.R. Lombardi and M. Leona, *Vibrational Spectrosc.*, 2009, **49**, 190-195.

48. T. Armaroli, M. Bevilacqua, M. Trombetta, A. G. Alejandre, J. Ramirez and G. Busca, *Appl. Catal. A*, 2001, **220**, 181-190.

49. R. Wendelbo, and R. Roque-Malherbe, *Microporous Materials*, 1997, **10**, 231-246.

50. T.C. Swinney and D.F. Kelley, *J. Chem. Phys.*, 1993, **99**, 211-221.

51. M. Hureau, K. Smirnov, A. Moissette and H. Jobic *Phys.Chem.Chem.Phys.*, 2014, **16**, 7562-7570.

52. J.P. Cornard, L. Vrielynck, J. C. Merlin and J. C. Wallet, *Spectrochim. Acta A*, 1995, **51A**, 913-23.

53. A. Moissette, Y. Batonneau, and C. Bremard, *J. Am. Chem. Soc.*, 2001, **123**, 12325-12334.

54. R.A. Marcus, *J. Chem. Phys.*, 1965, **43**, 679-701.

Figure caption

Fig. 1: 3-hydroxyflavone (3HF) predicted sorption site in straight channel of NaZSM-5. Red, yellow, and pink sticks represent the O, Si, and Al atoms of the framework, respectively. The white, shaded and red cylinders represent the H, C and O atoms of the 3HF molecule, respectively. The purple sphere represents the Na^+ cation.

Fig. 2: Nitrogen adsorption-desorption isotherms at -196°C on HZSM-5 and 3HF@HZSM-5. P is the pressure at the equilibrium and P_0 is the saturated vapor pressure.

Fig. 3: Diffuse reflectance UV-visible (DRUVv) spectra recorded for bulk solid 3HF (a) and for 3HF adsorbed in silicalite-1 (b), in NaZSM-5 (c), in HZSM-5 (d) and in ZnZSM-5 (e) six months after mixing 3HF and zeolite powders. The spectra are vertically shifted for the sake of better clarity.

Fig. 4: (A) FT-Raman spectra recorded for bulk solid 3HF (a) and for 3HF adsorbed in silicalite-1 (b), in NaZSM-5 (c), in HZSM-5 (d) six months after mixing 3HF and zeolite powders.
(B) FT-Raman spectra recorded for bulk solid 3HF (a) and for 3HF adsorbed in ZnZSM-5 (e) six months after mixing 3HF and zeolite powders.

Fig. 5: (A) FTIR spectra recorded in the 1250-1750 cm^{-1} spectral range for bulk solid 3HF (a) and for 3HF adsorbed in silicalite-1 (b), in NaZSM-5 (c), in HZSM-5 (d) and in ZnZSM-5 (e) six months after mixing 3HF and zeolite powders. The spectra of empty zeolites are given as references: NaZSM-5 (f), in HZSM-5 (g), silicalite-1 (h).
(B) FTIR spectra recorded in the 1420-1600 cm^{-1} spectral range for bulk solid 3HF (a) and for 3HF adsorbed in silicalite-1 (b), in NaZSM-5 (c), in HZSM-5 (d) and in ZnZSM-5 (e) six months after mixing 3HF and zeolite powders. The intensities of spectra (c) and (e) have been multiplied by 2 and 3, respectively for better comparison.

Fig. 6: Excitation emission spectra recorded for bulk solid 3HF (a) and for 3HF adsorbed in silicalite-1 (b), in NaZSM-5 (c), in HZSM-5 (d) and in ZnZSM-5 (e) six months after mixing 3HF and zeolite powders.

Fig. 7: (A) Time-resolved diffuse reflectance UV-vis (TRDRUVv) spectra collected at specified times following 355 nm laser excitation of 3HF@Na-ZSM-5 from 2 to 200 μs. (B) Normalized kinetic traces for the decay of the sample monitored at 480 nm following 355 nm laser excitation. The solid line represents the best-fit calculated decay using the Albery function; the squares represent the experimental points.

Fig. 8: (A) Time-resolved diffuse reflectance UV-vis (TRDRUVv) spectra collected at specified times following 355 nm laser excitation of 3HF@Zn-ZSM-5 from 1 to 200 μs. (B) Normalized kinetic traces for the decay of the sample monitored at 470 nm following 355 nm laser excitation. The solid line represents the best-fit calculated decay using the Albery function; the squares represent the experimental points. The solid line represents the best-fit calculated decay using the Albery function; the squares represent the experimental points.

Scheme 1: Mechanism of Excited State Intramolecular Proton Transfer (ESIPT) and Back Protn Transfer (BPT) for 3-hydroxyflavone (3HF).

Table 1 : Sample textural properties

Sample	BET surface area (m^2/g)	Microporous volume (cm^3/g)
HZSM-5	360	0.139
3HF@HZSM-5	312	0.125

Scheme 1.

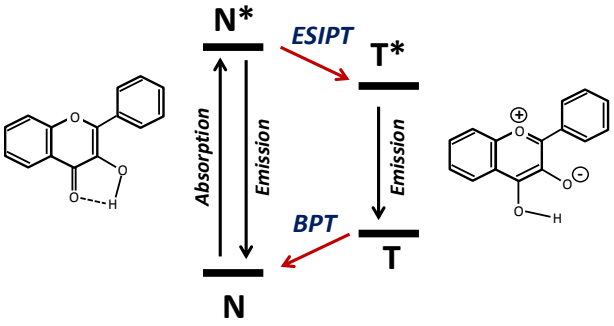

Fig. 1

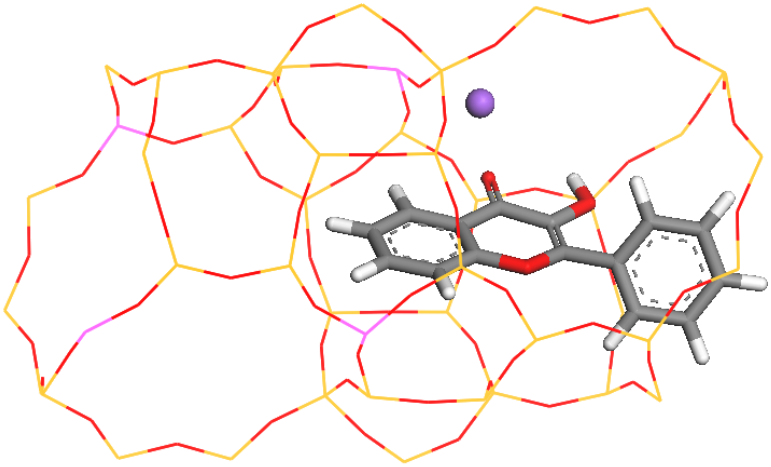

Fig. 2

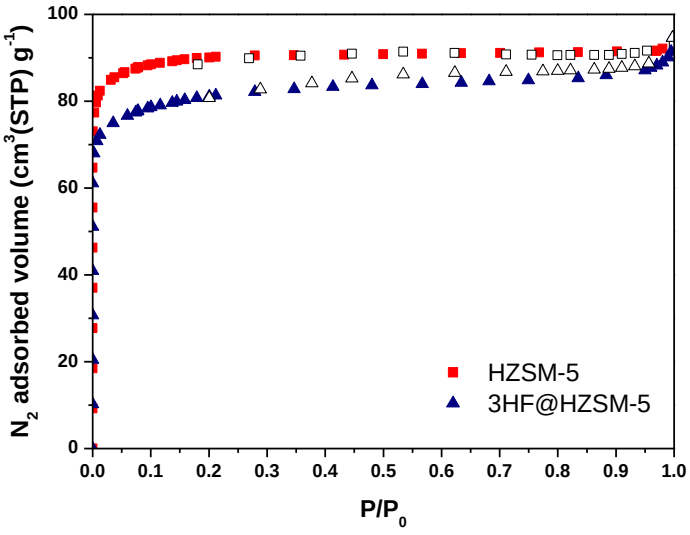

Fig. 3

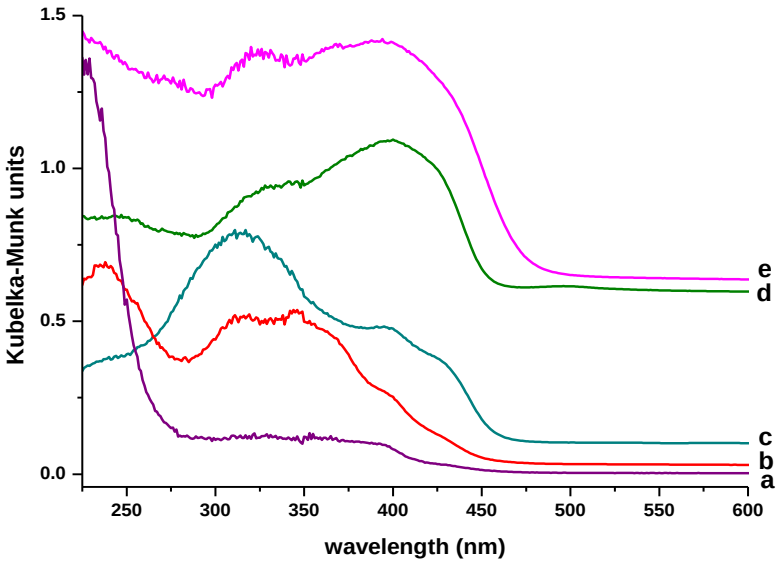

Fig. 4

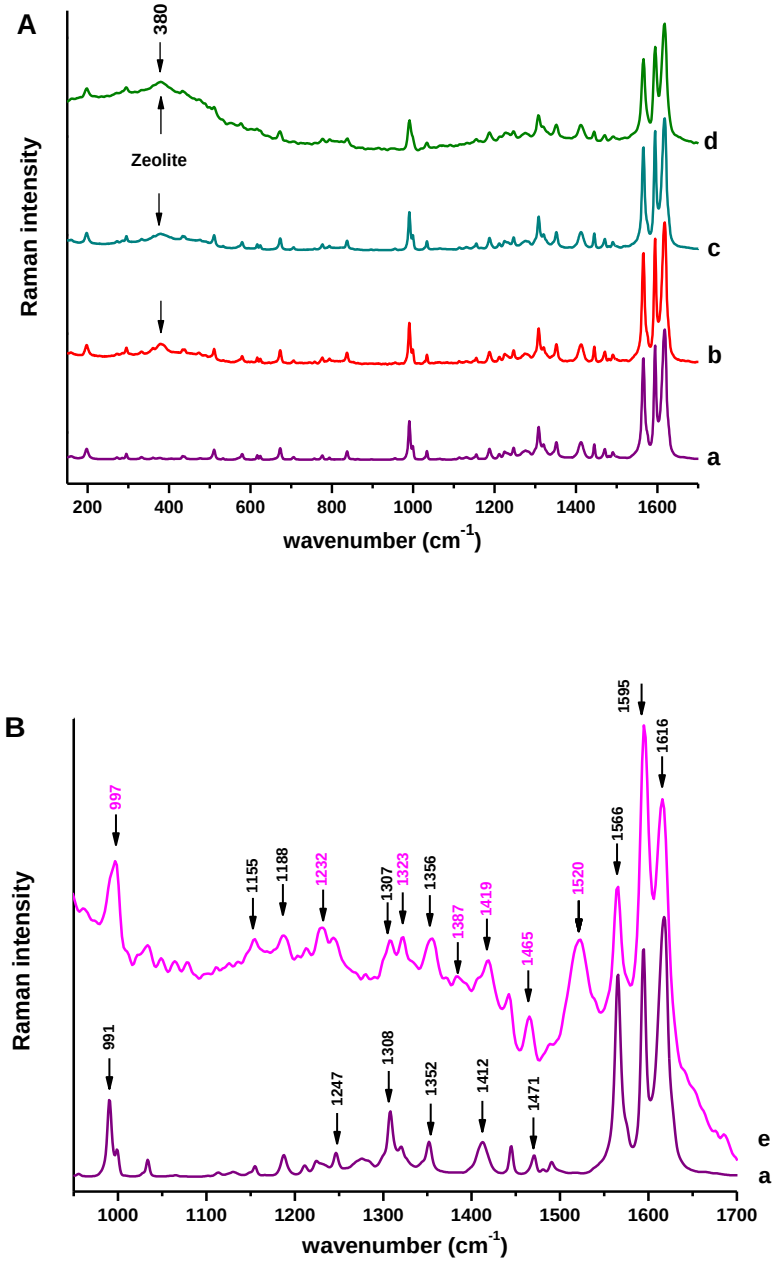

Fig. 5

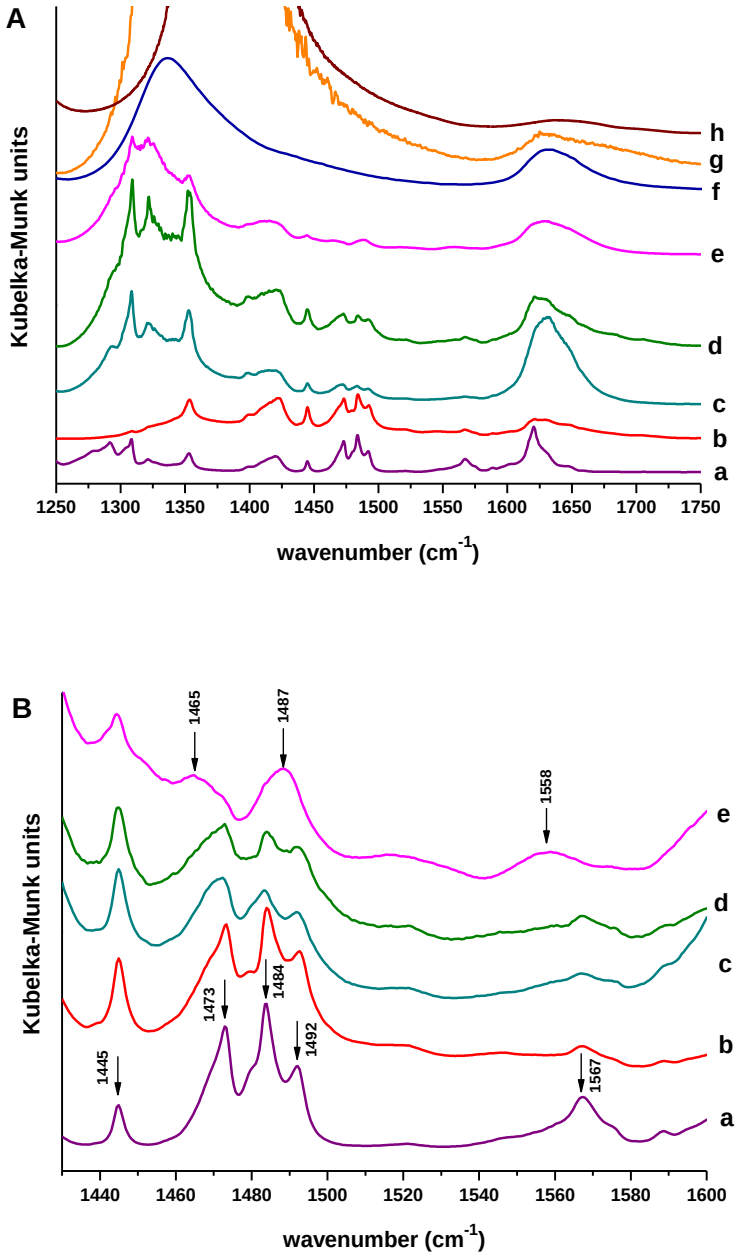

Fig. 6

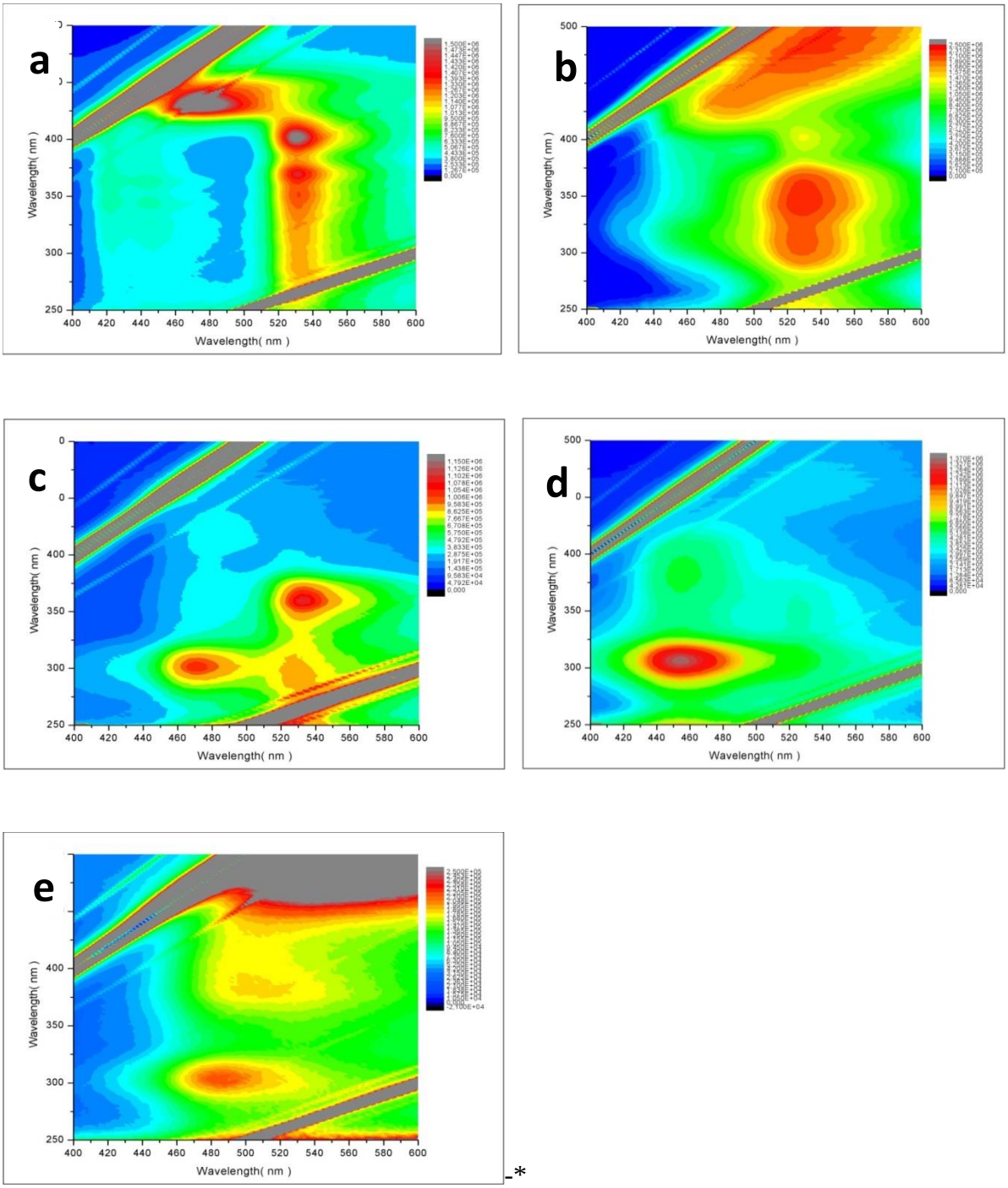

-*

Fig. 7

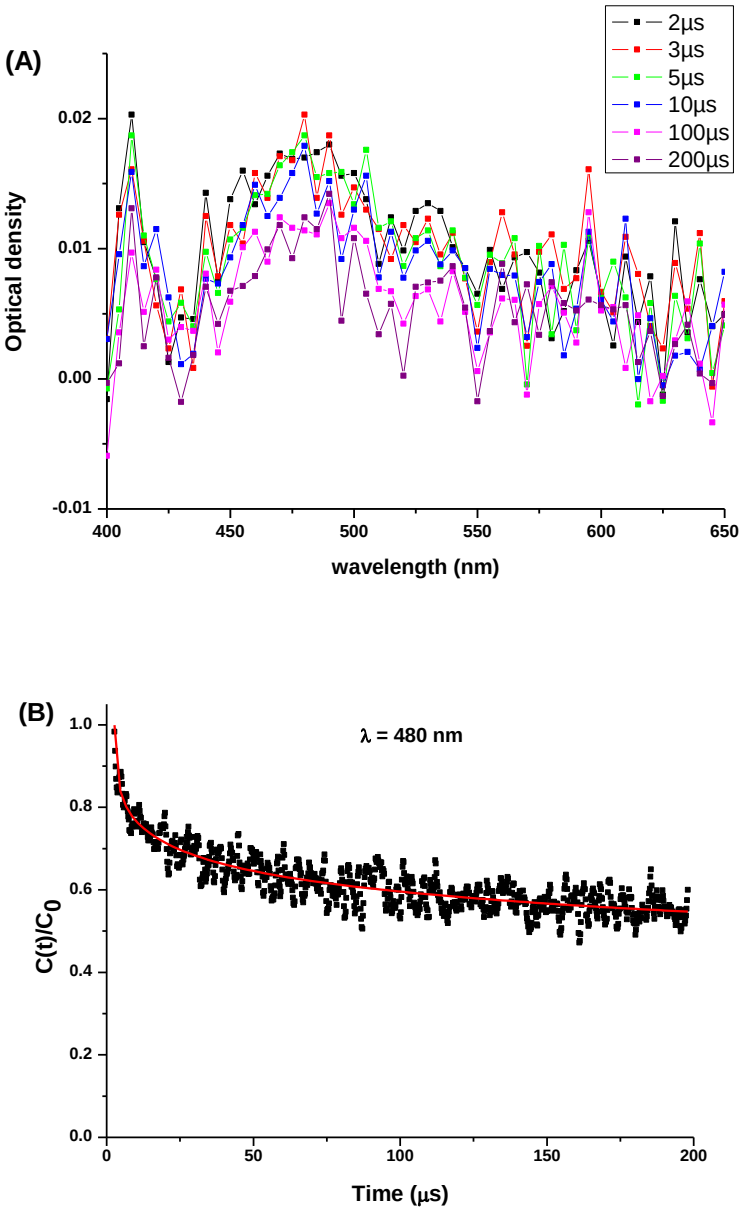

Fig. 8

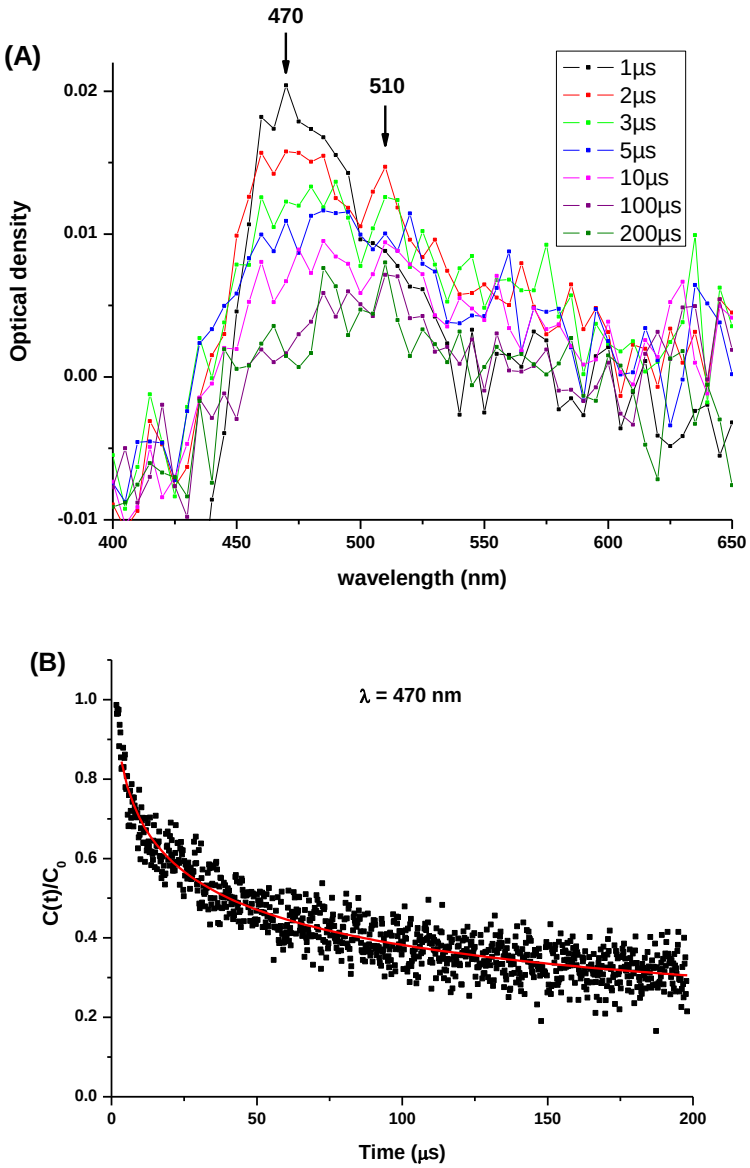

Graphical Abstract

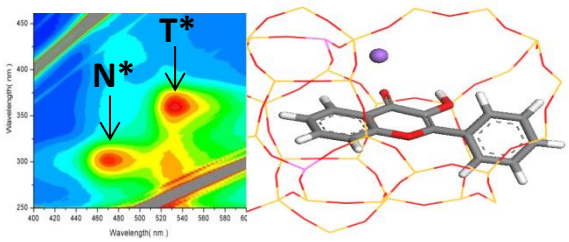

Spectroscopic evidence of 3-hydroxyflavone sorption within MFI type zeolites: ESIPT and metal complexation

A. Moissette,* [a] M. Hureau,[a] A. Kokaislova,[a,b] A. Le Person,[a] J.P. Cornard,[a] I. De Waele,[a] I. Batonneau-Gener[c]

Graphical abstract